

Fermi National Accelerator Laboratory

FERMILAB-Pub-94/211-T
SACLAY/SPhT-T94/94
DTP/94/62

The Same-Side/Opposite-Side Two-Jet Ratio

W. T. Giele

*Fermi National Accelerator Laboratory, P. O. Box 500,
Batavia, IL 60510. U.S.A.*

E. W. N. Glover

*Physics Department, University of Durham,
Durham DH1 3LE. England*

and

David A. Kosower

*Service de Physique Théorique, Centre d'Etudes de Saclay,
F-91191 Gif-sur-Yvette cedex. France*

August 1994

Abstract

We study the next-to-leading order QCD corrections to the same-side/opposite-side two jet ratio at Fermilab energies and show that the theoretical uncertainty on the factorization/renormalization scale is reduced. At large pseudorapidity the difference between the predictions for singular and non-singular distributions is 25% while the remaining scale uncertainty is significantly smaller than this.



One of the main ingredients for reliable predictions of hard scattering cross sections in proton-antiproton and electron-proton collisions is a precise knowledge of the density of gluons in the proton. However, unlike the charged parton distributions that are probed directly over a wide range of parton momentum fraction x and scale Q^2 in deeply inelastic scattering, the gluon density is only weakly constrained. The rather precise knowledge of the quark distributions does indicate how much of the proton's momentum is carried by gluons, but implies little about how the momentum is distributed. Only direct photon data from WA70 [1] constrains the shape of the gluon density in the $x \sim 0.3 - 0.4$ region. Recent measurements at HERA [2, 3] show that the F_2^{ep} structure function grows rapidly at small x ($x < \text{few} \times 10^{-3}$) which is due to the increase in the number of sea quarks, $xq_{\text{sea}} \sim x^{-0.3}$. Since the density of sea quarks at very low x is directly related to the density of gluons via the $g \rightarrow q\bar{q}$ process, this measurement suggests that $xg \sim x^{-0.3}$ at small x . However, although we expect this to be true as $x \rightarrow 0$, it is not clear at what value of x this behavior should set in. The uncertainty in the low x gluon distribution migrates to higher values of x via the momentum sum rule, and it is therefore crucial to attempt to make a direct measurement of the gluon density wherever possible and particularly at small x .

Recently, the CDF collaboration [4] has presented data for the ratio of same-side (SS) to opposite-side (OS) dijet production which, in principle, may be able to discriminate between a singular, $xg \sim x^{-0.5}$, and non-singular, $xg \sim x^0$, gluon distribution at small x . The reason for this is as follows. At lowest order, the transverse energies, $E_{T1} = E_{T2} = E_T$, and rapidities, η_1 and η_2 , of the two jets are directly related to the momentum fractions x_1 and x_2 of the incoming partons,

$$x_{1,2} = \frac{2E_T}{\sqrt{s}} \cosh(\eta^*) \exp(\pm\eta_{\text{boost}}), \quad (1)$$

where the rapidity of the two jet system in the laboratory frame is $\eta_{\text{boost}} = (\eta_1 + \eta_2)/2$ and the rapidity of the jet in the jet center of mass frame is $\eta^* = (\eta_1 - \eta_2)/2$. The lowest order cross section is given by,

$$\frac{d^3\sigma}{dE_T d\eta_1 d\eta_2} = \frac{1}{8\pi} \sum_{ij} x_1 f_i(x_1, \mu) x_2 f_j(x_2, \mu) \frac{\alpha_s^2(\mu)}{E_T^3} \frac{|\mathcal{M}_{ij}(\eta^*)|^2}{\cosh^4(\eta^*)}, \quad (2)$$

where $f_i(x, \mu)$ ($i = g, q, \bar{q}$) represents the density of parton i in the proton at factorization scale μ and $|\mathcal{M}_{ij}|^2$ are the lowest order squared matrix elements for $ij \rightarrow 2$ partons summed and averaged over initial and final state spins and colors ¹.

Same-side jets are defined to have $\eta_1 \sim \eta_2$ (i.e. $\eta^* \sim 0$) so that at large η and relatively small E_T , the same-side jet cross section probes the small x region. For example, for $\eta_1 = \eta_2 = 2.6$ and $E_T = 35$ GeV at $\sqrt{s} = 1800$ GeV, we find $x_1 = 0.52$ and $x_2 = 0.0029$, which indicates that the dominant contribution will come from the scattering of a valence quark off a gluon, $\sigma_{SS} \sim q_{\text{val}}(x_1)g(x_2)$. On the other hand, opposite-side jets are required to have

¹We have chosen the factorization scale μ_F and renormalization scale μ_R to be equal, $\mu_F = \mu_R = \mu$.

$\eta_1 \sim -\eta_2$ and $\eta_{\text{boost}} \sim 0$ so the opposite-side jet cross section occurs at roughly equal (and large) parton momentum fractions. For $\eta_1 = -\eta_2 = 2.6$ and $E_T = 35$ GeV, $x_1 = x_2 = 0.26$, where the parton distributions are relatively well known. Although the opposite-side cross section appears not to contain much new information, by taking the ratio,

$$R(\eta, E_T) \equiv \frac{\sigma_{SS}(\eta, E_T)}{\sigma_{OS}(\eta, E_T)}, \quad (3)$$

many of the theoretical and experimental uncertainties cancel out. For example, experimental uncertainties from the η dependence of the jet energy resolution and jet trigger efficiency are reduced in the ratio. On the theoretical front, much of the scale dependence and uncertainty in the strong coupling constant is reduced. In particular, at large η and small E_T ,

$$R(\eta, E_T) \sim g(x, \mu) F(\eta, E_T, \mu), \quad (4)$$

where $x = \frac{2E_T}{\sqrt{s}} \exp(-\eta)$ and this ratio may be a direct probe of the gluon density. The function $F(\eta, E_T, \mu)$ depends on parton distributions at moderate x values and is, in principle, reasonably well known. However, as noted by Martin, Roberts and Stirling (MRS) [5] a significant uncertainty still remains in the lowest order theoretical prediction, particularly at small E_T ². In general, the inclusion of next-to-leading order effects can reduce the theoretical uncertainty in three distinct ways. First there is some dependence on the jet algorithm, since two partons may now merge to form a jet. Second, the dependence on the renormalization and factorization scales is reduced. Third, certain kinematic constraints may be removed by the presence of an additional parton. Taken together, we might expect that by including the full next-to-leading order $\mathcal{O}(\alpha_s^3)$ QCD corrections the theoretical uncertainty on the ratio $R(\eta, E_T)$ might be reduced and that is the subject of this Letter.

To compute the next-to-leading order cross section we use an $\mathcal{O}(\alpha_s^3)$ Monte Carlo program for one, two and three jet production based on the one-loop $2 \rightarrow 2$ [7, 8] and the tree level $2 \rightarrow 3$ parton scattering amplitudes described in ref. [9]. This program uses the techniques of refs. [10, 11] to cancel the infrared and ultraviolet singularities thereby rendering the $2 \rightarrow 2$ and $2 \rightarrow 3$ parton processes finite and amenable to numerical computation. The parton four momenta are then passed through a jet algorithm to determine the one, two and three jet cross sections according to the experimental cuts. Different cuts and/or jet algorithms can easily be applied to the parton four-momenta and, in principle, any infrared-safe distribution computed at $\mathcal{O}(\alpha_s^3)$.

In order to compare the theory with experiment, we use the parton level equivalent of the so-called ‘Snowmass’ algorithm [12] with $\Delta R = 0.7$ and require at least two jets in the event. Same-side events are identified as events where the rapidities of the two leading jets in transverse energy lie in the same rapidity bin, $\eta - \Delta\eta < \eta_1, \eta_2 < \eta + \Delta\eta$ with $\Delta\eta = 0.2$ while for the opposite-side cross section, $\eta - \Delta\eta < |\eta_1|, |\eta_2| < \eta + \Delta\eta$ but the signs of η_1 and η_2

²In that paper, the authors have tried to mimic the next-to-leading order results by using the particular scale choice $\mu = \cosh(\eta^*)/\cosh(0.7\eta^*)E_T/2$ as motivated by ref. [6]. As a result, the factorization/renormalization scale used for the same-side ($\eta^* \sim 0$) and opposite-side ($|\eta^*| > 0$) are rather different.

are opposite. At a given factorization/renormalization scale μ , the same-side/opposite-side cross sections are thus,

$$\sigma_{SS}(\eta, \mu) = \int_{\eta-\Delta\eta}^{\eta+\Delta\eta} d\eta_1 \int_{\eta-\Delta\eta}^{\eta+\Delta\eta} d\eta_2 \int_{E_{T\min}}^{E_{T\max}} dE_T \frac{d^3\sigma(\mu)}{dE_T d\eta_1 d\eta_2}, \quad (5)$$

$$\sigma_{OS}(\eta, \mu) = \int_{\eta-\Delta\eta}^{\eta+\Delta\eta} d\eta_1 \int_{-\eta-\Delta\eta}^{-\eta+\Delta\eta} d\eta_2 \int_{E_{T\min}}^{E_{T\max}} dE_T \frac{d^3\sigma(\mu)}{dE_T d\eta_1 d\eta_2}. \quad (6)$$

for a transverse energy interval $E_{T\min} < E_T < E_{T\max}$. Since the assignment of which jet is hardest is not an infrared safe quantity [9], the roles of the leading and next-to-leading transverse energy jets must be interchanged so that each event is effectively counted twice. In addition, the two leading jets must be well separated in azimuth $\pi - 0.7 < \Delta\phi < \pi + 0.7$ [4].

To focus on the gluon density at small x , we use the improved MRSD– and MRSD0 distributions of ref. [13] for which xg behave as $x^{-0.5}$ and x^0 , respectively at small x and low Q^2 . Although the low- x behavior of F_2^{eP} as measured at HERA is better fitted by an $x^{-0.3}$ behavior [14], the range of predictions from MRSD– and MRSD0 indicate the level of experimental/theoretical accuracy necessary to constrain the gluon density with the same-side/opposite-side jet ratio. Furthermore, we use the running *one*-loop strong coupling constant α_s , in calculating the leading-order predictions, and the two-loop running coupling constant for the next-to-leading order predictions. In both cases, we take $\Lambda_{QCD}^{(4)} = 230$ MeV as specified by the structure function parametrization, so that $\alpha_s^{(1)}(M_Z) = 0.131$ and $\alpha_s^{(2)}(M_Z) = 0.111$. Alternatively, we could preserve $\alpha_s^{(1)}(M_Z) = \alpha_s^{(2)}(M_Z) = 0.111$ by adjusting the value of $\Lambda_{QCD}^{(4)} \rightarrow 82$ MeV used in the lowest order calculation. Both approaches are equivalent at lowest order and reflect part of the theoretical uncertainty present at this order in perturbation theory. Equally, the use of parton densities with next-to-leading order evolution in the leading order cross section is consistent at $\mathcal{O}(\alpha_s^2)$.

The leading and next-to-leading order same-side/opposite-side cross sections, $\sigma_{SS}(\eta, \mu)$ and $\sigma_{OS}(\eta, \mu)$ are shown in fig. 1 for the MRSD– parton densities and the renormalization/factorization scale equal to the hardest jet in the event, $\mu = E_T$. As expected, the SS and OS cross sections are symmetric under $\eta \leftrightarrow -\eta$, and are approximately equal in the region $\eta \sim 0$. It is interesting to ask why the SS and OS cross sections have such a different behavior as $|\eta|$ increases. At fixed E_T , the lowest order parton level matrix elements depend only on η^* . For example, for the $gg \rightarrow gg$ subprocess,

$$|\mathcal{M}|^2 \sim \frac{(4 \cosh^2(\eta^*) - 1)^3}{\cosh^2(\eta^*)}. \quad (7)$$

In the same-side cross section, $\eta^* \sim 0$ so the parton level matrix elements are roughly constant. This is modified by the parton densities which drop rapidly as $|\eta|$ increases so that the same-side cross section falls off monotonically with $|\eta|$. On the other hand, in the opposite-side cross section, $\eta^* \sim \eta$ so that the parton level matrix elements increase with $|\eta|$. This growth is most marked at small $|\eta|$, where it dominates the falling parton luminosity.

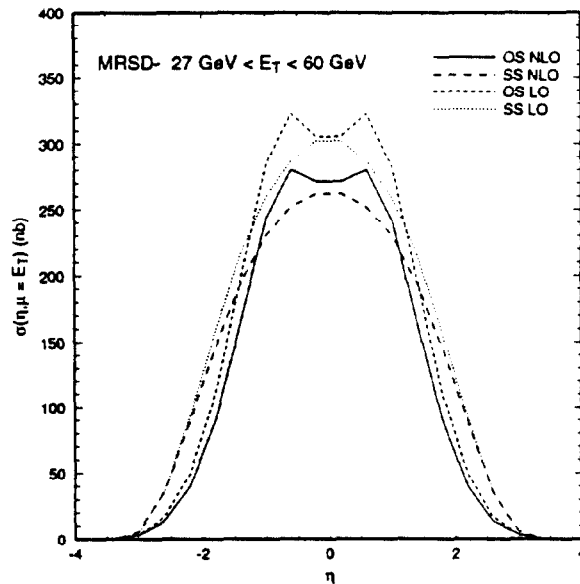


Figure 1: The leading (LO) and next-to-leading order (NLO) predictions for the same-side (SS) and opposite-side (OS) cross sections as a function of η for $27 \text{ GeV} < E_T < 60 \text{ GeV}$, $\mu = E_T$ and the MRSD- structure functions.

The opposite-side cross section therefore increases with $|\eta|$ for small $|\eta|$. However, at larger values of $|\eta|$, the dropping parton luminosity ensures that the opposite-side cross section decreases at large $|\eta|$. As a result, the opposite-side cross section peaks away from $\eta = 0$.

Fig. 1 shows that, for this choice of parameters, the next-to-leading order corrections are not large. While the absolute normalization of the lowest order cross section is rather uncertain³ the main point to note is that the shape of the cross section is only slightly changed by the inclusion of the next-to-leading order corrections. This is more clearly seen in fig. 2 which shows the ratio of next-to-leading order to leading order SS and OS cross sections. For $|\eta| < 3$ we see that the corrections are essentially independent of $|\eta|$ which gives us confidence that the SS and OS cross sections are reliably computed in perturbation theory. For very large $|\eta|$, the corrections are somewhat larger. For $E_T = 27 \text{ GeV}$ and $\sqrt{s} = 1800 \text{ GeV}$, the leading-order OS cross section has a kinematic limit of $|\eta| < \cosh^{-1}(\sqrt{s}/2E_T) = 4.2$, while the SS cross section is restricted to $|\eta| < \log(\sqrt{s}/2E_T) = 3.5$. These limits are relaxed at next-to-leading order, which includes $2 \rightarrow 3$ processes, so the corrections are large. As discussed in ref. [9], however, this does *not* signal the emergence of large logarithms which might spoil the applicability of perturbation theory.

As discussed above, the kinematic region most sensitive to the gluon distribution is at large η and small E_T . Fig. 3 shows the scale dependence of the leading order and next-to-leading order predictions for the same-side and opposite-side cross sections at Fermilab

³For example, adjusting $\Lambda_{QCD}^{(4)} \rightarrow 82 \text{ MeV}$ increases the lowest order cross sections by $\mathcal{O}(40\%)$

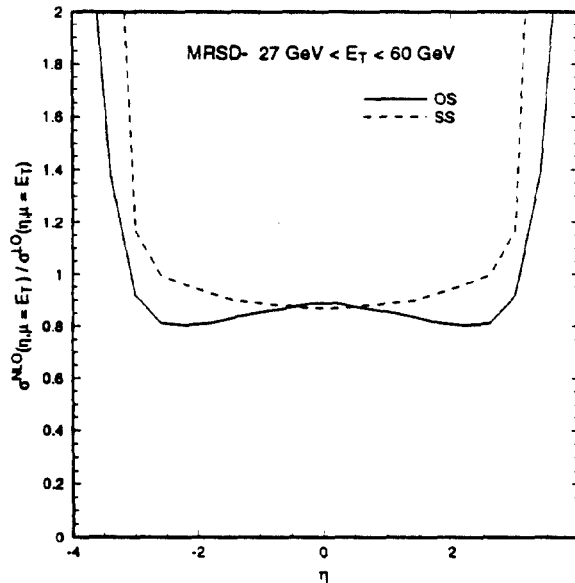


Figure 2: The ratio of next-to-leading order (NLO) to leading order (LO) predictions for the same-side (SS) and opposite-side (OS) cross sections as a function of η for $27 \text{ GeV} < E_T < 60 \text{ GeV}$, $\mu = E_T$ and the MRSD– structure functions.

energies for $\eta = 2.6$ and $27 \text{ GeV} < E_T < 60 \text{ GeV}$. We see that the scale dependence is reduced by including the next-to-leading order corrections. In fact, the next-to-leading order corrections approximately vanish for the same-side distribution at $\mu = E_T$ and at $\mu \sim 2E_T$ for the opposite-side distribution. This is in rough agreement with the approximate form (extended beyond its kinematic range of validity by MRS [5]) given in ref. [6], which suggests that the next-to-leading order corrections are small at this value of η when $\mu_{OS} \sim 2.13\mu_{SS}$.

One of the motivations for studying the SS/OS ratio is that most of the experimental and theoretical uncertainties cancel. The differing calorimetric response as $|\eta|$ varies can be largely eliminated since there is an approximate forward/backward symmetry of the detector. Similarly, the theoretical uncertainty due to the strong coupling constant is reduced (and removed at lowest order if $\mu_{SS} = \mu_{OS}$), although some factorization scale dependence remains. This ratio is shown in fig. 4 for the same values of η and E_T used in fig. 3. We see that the rather steeply falling behavior of the individual leading-order SS and OS cross sections shown in fig. 3 has been completely reversed; the leading-order ratio between the two increases with the renormalization/factorization scale. This reflects the increase of parton luminosity with factorization scale for these x values. As expected, the scale dependence of the next-to-leading order prediction is rather flat over this range of μ , showing that the inclusion of the $\mathcal{O}(\alpha_s^3)$ corrections has reduced the theoretical uncertainty. For $\mu \sim E_T$, the ratio of cross sections is almost insensitive to the choice of μ .

Finally, in fig. 5, we show the predictions for the full range of η with $\mu_{SS} = \mu_{OS}$. For comparison we also show the data points from the preliminary CDF measurement [4] for jets

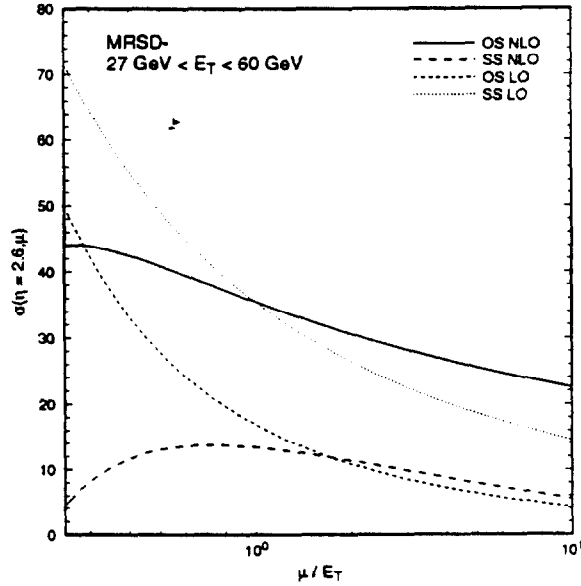


Figure 3: The next-to-leading order (NLO) to leading order (LO) predictions for the same-side (SS) and opposite-side (OS) cross sections as a function of μ/E_T for $27 \text{ GeV} < E_T < 60 \text{ GeV}$, $\eta = 2.6$ and the MRSD– structure functions.

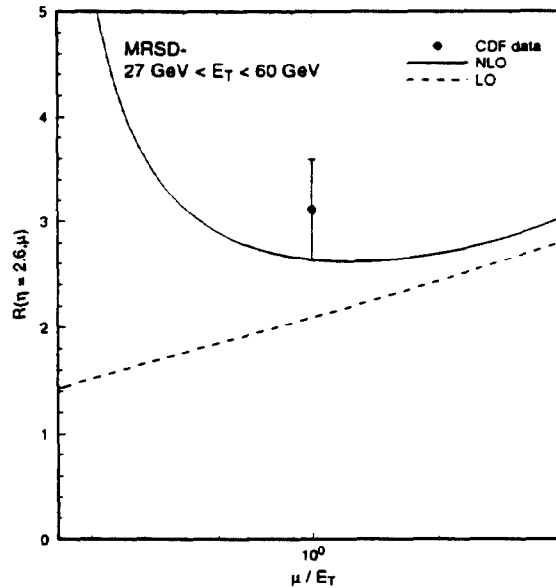


Figure 4: The scale variation of the ratio of same-side (SS) and opposite-side (OS) cross sections at $\eta = 2.6$ at next-to-leading order (NLO) and leading order (LO) for $27 \text{ GeV} < E_T < 60 \text{ GeV}$ and the MRSD– structure functions. The data point is taken from [4].

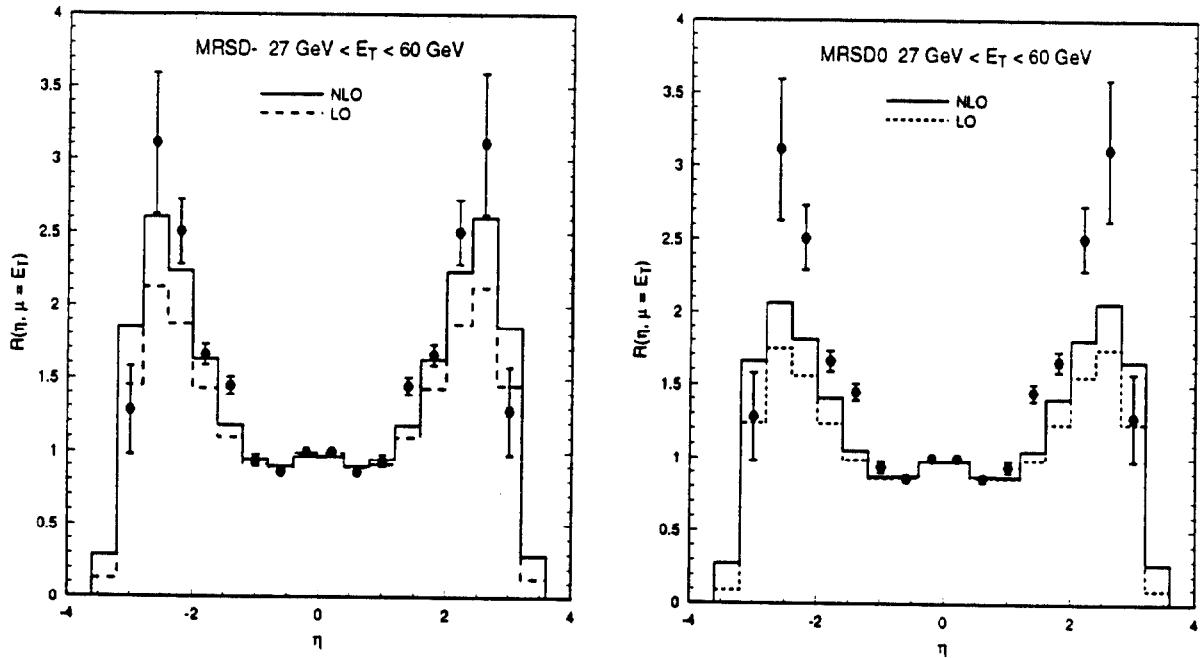


Figure 5: The ratio of same-side (SS) and opposite-side (OS) cross sections at next-to-leading order (NLO) and leading order (LO) as a function of η for $27 \text{ GeV} < E_T < 60 \text{ GeV}$, $\mu = E_T$ and (a) MRSD- (b) MRSD0 structure functions. The data is taken from [4].

with $27 \text{ GeV} < E_T < 60 \text{ GeV}$. We see that the next-to-leading order corrections move the theory closer to the data. We also note that the difference between the singular and non-singular gluon density (MRSD- and MRSD0) corresponds to a difference of approximately +25% in the ratio at $\eta = 2.6$ which is much larger than the uncertainty due to the factorization/renormalization scale. The preliminary data, with admittedly large errors, already appears to favour the more singular gluon density. With more data it should prove possible to make a determination of the low x gluon density from the same-side/opposite-side dijet cross section.

Acknowledgements

We thank Alan Martin for valuable discussions. EWNG thanks the Fermilab Theory group, where part of this work was carried out, for its kind hospitality.

References

- [1] WA70 Collaboration, M. Bonesini *et al*, Z. Phys. **C38** 371 (1988).
- [2] H1 Collaboration, I. Abt *et al*, Nucl. Phys. **B407** 515 (1993).
- [3] ZEUS Collaboration, M. Derrick *et al*, Phys. Lett. **B316** 412 (1993).
- [4] CDF Collaboration, F. Abe *et al*, Fermilab preprint, FERMILAB-CONF-93/203-E: CDF Collaboration, presented by Eve Kovacs, Eighth Meeting of the Division of Particles and Fields of the American Physical Society, Albuquerque, New Mexico, August 1994.
- [5] A.D. Martin, R.G. Roberts and W.J. Stirling, Phys. Lett. **B318** 184 (1993).
- [6] S. D. Ellis, Z. Kunszt and D. E. Soper, Phys. Rev. Letts. **69**, 1496 (1992).
- [7] R. K. Ellis and J. Sexton, Nucl. Phys. **B269**, 445 (1986).
- [8] Z. Bern and D. A. Kosower, Nucl. Phys. **B379**, 451 (1992); Z. Kunszt, A. Signer, and Z. Trocsanyi, Nucl. Phys. **B411**, 397 (1994).
- [9] W. T. Giele, E. W. N. Glover and D. A. Kosower, Fermilab preprint, FERMILAB-Pub-94/070-T.
- [10] W. T. Giele and E. W. N. Glover, Phys. Rev. **D46**, 1980 (1992).
- [11] W. T. Giele, E. W. N. Glover and D. A. Kosower, Nucl. Phys. **B403**, 633 (1993).
- [12] See, for example, J.E. Huth *et al.*, in Research Directions for the Decade, Proceedings of the 1990 Division of Particles and Fields Summer Study, Snowmass, 1990, edited by E.L. Berger (World Scientific, Singapore, 1992), p.134.
- [13] A. D. Martin, R. G. Roberts and W. J. Stirling, Phys. Letts. **B306**, 145 (1993).
- [14] A. D. Martin, R. G. Roberts and W. J. Stirling, Durham preprint DTP/94/34, Rutherford preprint RAL-94-55.